48th International Liège Colloquium: Submesoscale Processes: Mechanisms, Implications and New Frontiers. May 2016.

Investigating SWOT capabilities to detect submesoscale eddies in the Canary Islands: application of the SWOT simulator

Laura Gómez-Navarro[1], Evan Mason[2] and Ananda Pascual[2]
[1]Université de la Bretagne Occidentale, Brest, France.
[2]Institut Mediterrani d'Estudis Avançats, IMEDEA (CSIC-UIB), Mallorca, Spain.
Contact: lauragomnav@gmail.com

1. Introduction

The joint National Aeronautics and Space Administration (NASA), *Centre National d'Études Spatiales* (CNES) and Canadian Space Agency (CSA) [Alsdorf *et al*., 2011] Surface Water and Ocean Topography (SWOT) satellite mission is now planned to be launched in 2020. Fig.1 shows some of the satellite's characteristics. It will measure wide-swath Sea Surface Height (SSH) at a higher spatial resolution than present day satellites [Fu and Ferrari, 2008], for e.g. in fig. 2, JASON2 and SWOT tracks are compared.

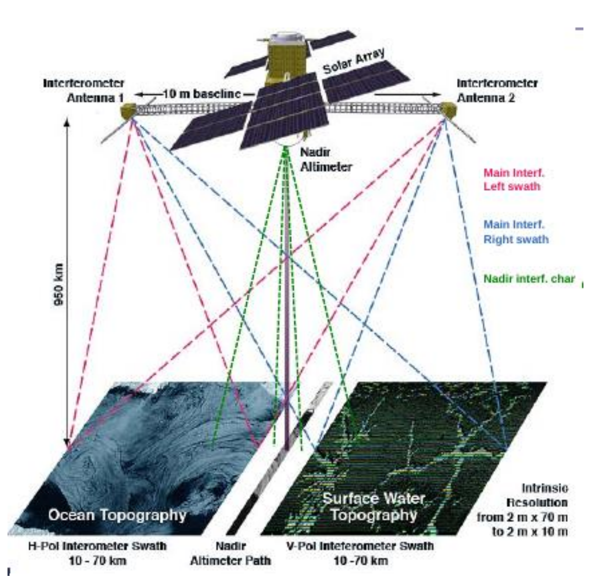

Fig. 1. SWOT satellite characteristics [L.L. Fu, oral communication]

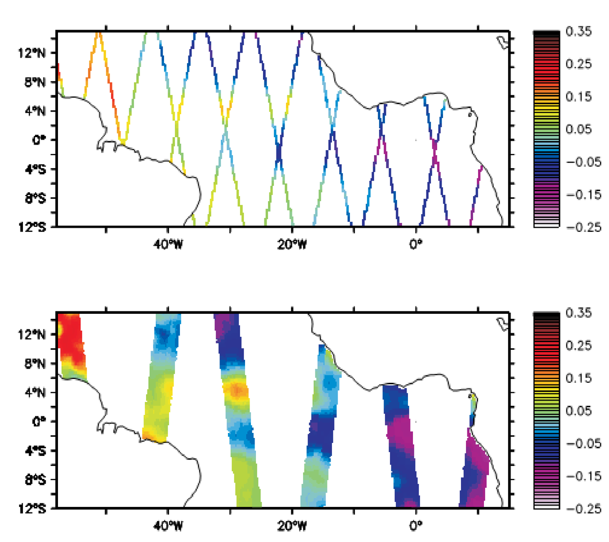
Fig. 2. Along-track SSH (m) extracted from days 30 to 33 of a simulation. Upper panel: JASON2. Lower panel: SWOT. [Pujol *et al.*, 2012].

In this study we use the SWOT simulator with the objectives:

1. To understand the future data from the SWOT satellite.
2. To detect anticyclonic eddies identified in a submesoscale resolving Regional Ocean Modeling System (ROMS) solution (fig. 3).

Similar structures have been identified near the coast by Bassin *et al*., [2005], in the southern California Bight. In our case, they are shed by a cape (La Isleta) at the northeast of the island of Gran Canaria. These La Isleta Shedded Eddies (LISE) have been identified in the outputs of simulations of the Canary Islands region [Mason, 2010], and increase in size as they move south. Their diameters range from about 4 km (eddy A3 in fig. 3) to 10 km (A5). They may help explain nutrient and planktonic distributions in the area, by producing cross-isobath transport along the slope [Bassin *et al*., 2005].

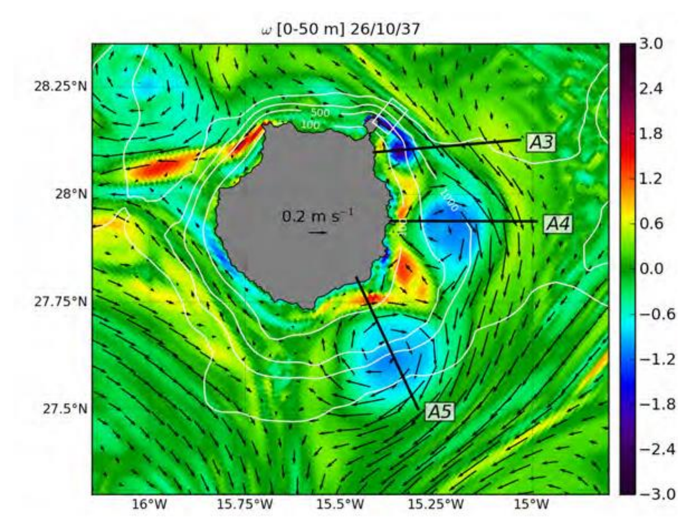

Fig. 3. Snapshot of normalised (by f) depth-averaged (0 - 50 m) relative vorticity at Gran Canaria. Black arrows show the current velocity. A3, A4 and A5 are a sequence of anticyclonic eddies. [Mason, 2010].

2. Materials and methods

2.1. The SWOT simulator

The SWOT simulator, developed by the California Institute of Technology, is a relatively recent numerical tool that provides statistically reliable SSH outputs of what the satellite should measure. Therefore, the existence of the simulator makes it possible to start optimization of information retrieval protocols/procedures for the processing of future SWOT data. [Gaultier et al., 2016]. This software generates SWOT-like outputs on a swath along the orbit ground track, by:

1. It generates the grid files corresponding to the domain and orbit specified.
2. The model input data is linearly interpolated in space [Gaultier and Ubelmann, 2015] into the SWOT grid.
3. The simulated SSH is obtained for each possible path in the specified space and time domains.
4. Using recent technical characteristics established by the SWOT project team, measurement error and noise are added.

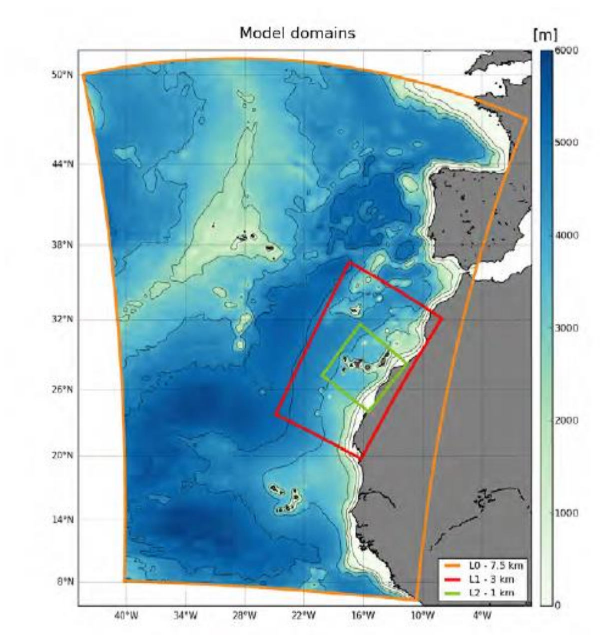

Fig. 4. The nested model domains: L0, L1 and L2. The topography for each grid is shown. Isobaths from L0 are plotted at 200, 1000, 2500, 4000 and 5000 m. [Mason, 2010]

2.2. The ROMS input data

As the LISEs are observed in the Canary Islands' ROMS simulation (fig. 4) it is used as the model input data for the SWOT simulator. This one-way nested ROMS configuration represents a full seasonal cycle at a high enough spatial resolution (1 km) to observe submesoscale structures.

2.3. Satellite data

2.3.1. Sea Surface Temperature (SST)

The Multi-scale ultra-high resolution (MUR) L4 SST analysis has a global spatial resolution of 0.01º. It is obtained by optimally interpolating and merging the data from the AVHRR, MODIS and AMSR-E sensors. (https://podaac.jpl.nasa.gov/dataset/JPL-L4UHfnd-GLOB-MUR)

2.3.2. Chlorophyll

Several ocean colour satellite datasets were analyzed. In this poster the L3 data from the Visible Infrared Imager/Radiometer Suite (VIIRS) are shown. It is the successor to MODIS, and provides global chlorophyll concentration at a spatial scale of 4km. (http://oceancolor.gsfc.nasa.gov/cms/data/viirs)

3. Results

3.1. Preliminary results

Firstly, several SWOT simulations were done to explore and test a range of optimum parameters to correctly run the simulator for our region of interest. One of the figures obtained was fig. 5, in which SWOT's high spatial coverage can be seen, and mesoscale structures can be clearly observed. To get an idea of the order of the passes and the relevance of the time between them spatially, the time of the passes was plotted (fig. 6).

Errors in the SSH simulated could occur if one of the swaths in the domain coincided with the transition time between 2 time steps. Fig. 6 showed that in our case, this error was not present.

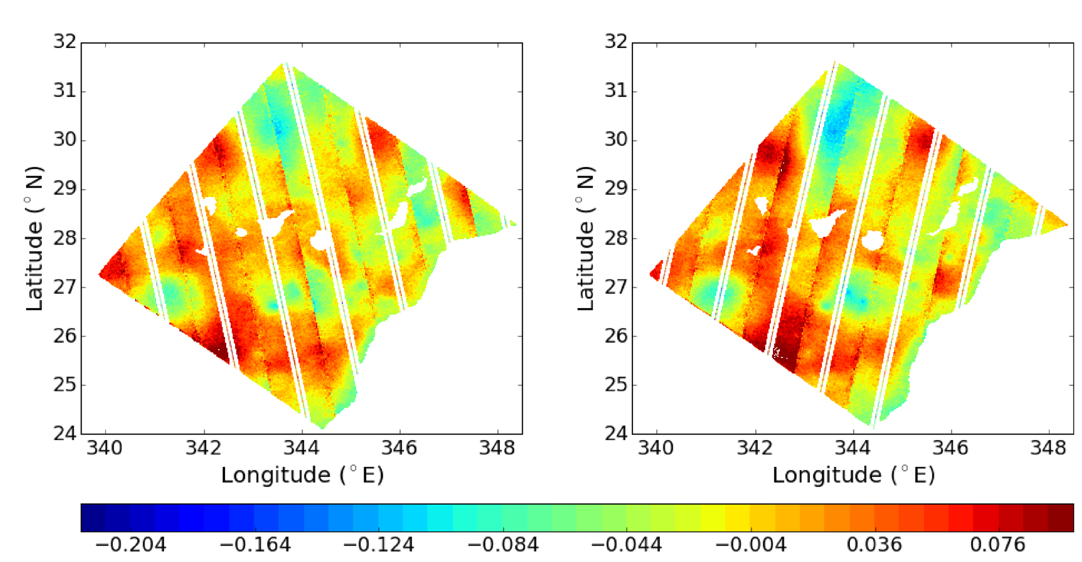

Fig. 5. SWOT simulator SSH (m) composite figure of the first cycle's passes (separated in ascending/descending tracks).

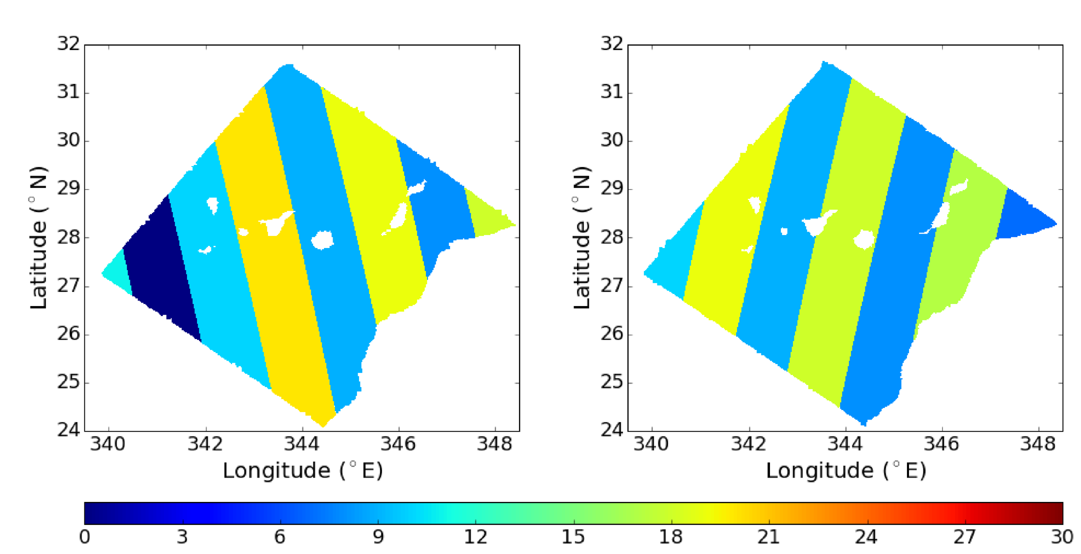

Fig. 6. Time from the beginning of the simulation (days) for the first cycle's passes (separated in ascending/descending tracks).

3.2. LISEs detection

3.2.1. ROMS files

The SSH ROMS outputs were analyzed to determine the temporal and spatial occurrence of these eddies. A table of the temporal occurrence was done to then obtain the corresponding SWOT simulator outputs. In table 1, it can be observed how the LISEs' frequency is very low, and although less than 2 years were analyzed, it seems to have no clear pattern [Mason, 2010]. Nevertheless, the LISEs detected refer only to the ones generated from a northwestward flow, but also eddies shedded from a flow in the opposite direction could be observed. In this case, they were cyclonic eddies instead of anticyclonic, as expected.

Table 1: Presence of the LISEs during the first 14 months of the ROMS SSH outputs, shown by a clockwise dark blue arrow (corresponding to the anticyclonic LISEs).

	Day 1	2	3	4	5	6	7	8	9	10	11	12	13	14	15	16	17	18	19	20	21	22	23	24	25	26	27	28	29	30
Month 1																										↻	↻	↻	↻	↻
2	↻	↻	↻	↻	↻	↻	↻	↻	↻	↻	↻																			
3			↻	↻	↻	↻	↻																							
4																														
5																														
6																														
7																														
8																														
9																														
10																														
11																														
12																	↻	↻	↻	↻	↻	↻	↻	↻	↻	↻	↻	↻	↻	↻
13	↻	↻	↻	↻	↻	↻	↻	↻	↻	↻	↻	↻	↻	↻																
14	↻	↻	↻	↻	↻	↻	↻	↻	↻	↻	↻	↻	↻	↻	↻	↻	↻	↻	↻	↻	↻	↻	↻	↻	↻	↻	↻	↻	↻	

3.2.2. Satellite images

LISEs type structures have also been identified in other satellite images of SST anomalies (fig. 7, left) and of chlorophyll (fig. 7, right), but LISEs have never been measured *in situ*. This is probably due to their sampling difficulty given their small spatial and temporal scales.

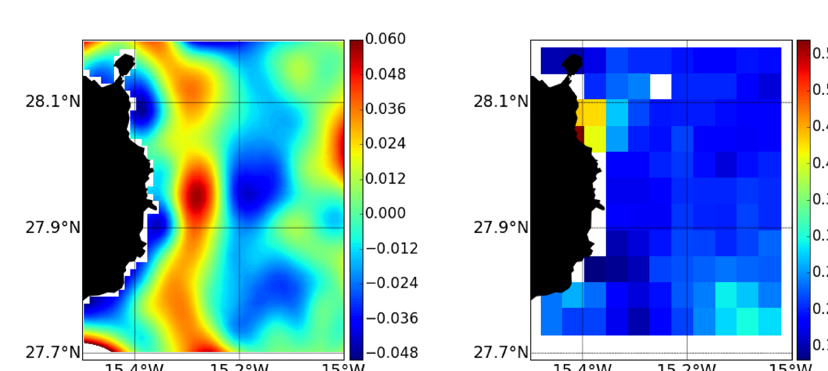

Fig. 7. MUR SST anomaly in ºC (left) and chlorophyll in mg/m³ (right) on the 6th of January 2003.

3.2.3. SWOT simulator

Using table 1, the corresponding SWOT simulator swaths for when LISEs were observed were plotted. For example, using day 51 of the ROMS files, interpolated into the SWOT grid (fig. 8a), the pseudo-SWOT swath corresponding to pass 133 of cycle 3 was obtained (fig 8b). Unfortunately, like with other interesting satellite passes, it has the nadir track covering the region where LISEs are identified. Consequently, one of the simulator's parameters, the longitude shift, was used to obtain swaths where the region of interest was visible (figs. 8c and d).

In figures 8b and d it can be observed how the simulated SSH is quite noisy. If the added noise corresponding to these figures is simulated one can see that it is high (fig. 8e) compared to the magnitude of the simulated SSH.

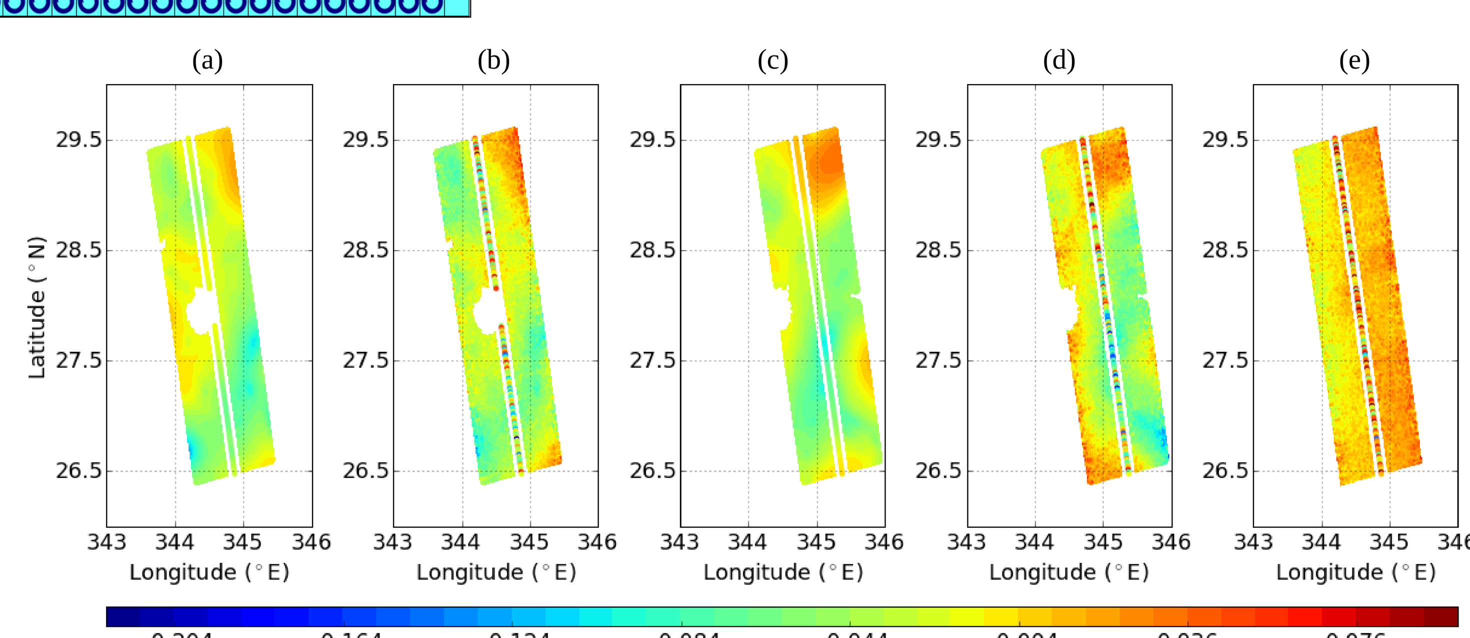

Fig. 8. Swaths for cycle 3 pass 133 (m). SSH model (a) and simulated data (b) with a longitude shift of 0.5º (c, d model and simulated data respectively), and the simulator added noise (e).

4. Conclusions and perspectives

- Outputs of the SWOT simulator were obtained for the Canary Islands region, a preliminary step in trying to detect the submesoscale eddies of interest.
- It is necessary to implement interpolation techniques, like the dynamic interpolation proposed by Ubelmann *et al*. [2015] due to the low temporal scales of the submesoscale structures. Also spatial interpolation is necessary [Gaultier *et al*., 2016] due to the satellite's noise.
- In future work, other submesoscale eddies around the islands could be studied, the time shift and other parameters of the simulator could be varied in order to detect these submesoscale features more often.
- Moreover, we have started to carry out simulations in the western Mediterranean where the range of SSH values is greater than at the Canary Islands, and thus we expect the impact of the simulator added noise to be lower.

References:

*Alsdorf, D. E., Mognard, N. M., Lettenmaier, D. P. and SWOT Virtual Mission Team, 2011. Remote Sensing of Surface Water and Recent Developments in the SWOT Mission. *AGU Fall Meeting Abstracts*, page J6.
*Bassin, C. J., Wasburn, L., Brzezinski, M. and McPhee-Shaw, E., 2005. Sub-mesoscale coastal eddies observed by high frequency radar: A new mechanism for delivering nutrients to kelp forests in the Southern California Bight. *Geophysical Research Letters*, 32(12).
*Fu, L. L. and Ferrari, R., 2008. Observing Oceanic Submesoscale Processes From Space. *Eos Trans. AGU*, 89(48), 488-488.
*Fu, L. L. Surface Water Ocean Topography (SWOT) Mission. Oral communication.
*Gaultier, L. and Ubelmann, C., 2015. SWOT Simulator Documentation. Technical report. Release 1.0.0.
*Gaultier, L., Ubelmann, C. and Fu, L. L., 2016. The challenge of using future swot data for oceanic field reconstruction. *J. Atmos. Oceanic Technol*., 33, 119–126.
*Mason, E., Molemaker, J., Shchepetkin, A., Colas, F., McWilliams, J. C. and Sangrà, P., 2010. Procedures for offline grid nesting in regional ocean models. *Ocean modelling*, 35, 1–15.
*Mason, E. High-resolution modelling of the Canary Basin oceanic circulation. *PhD thesis, Universidad de Las Palmas de Gran Canaria*, 2009. 245pp.
*Pujol, M.-I., Dibarboure, G., Le Traon, P.-Y. and Klein, P., 2012. Using High-Resolution Altimetry to Observe Mesoscale Signals. *Journal of Atmospheric and Oceanic Technology*, 29, 1409-1416.
*Ubelmann, C., Klein, P. and Fu L.L., 2015. Dynamic Interpolation of Sea Surface Height and Potential Applications for Future High-Resolution Altimetry Mapping. *Journal of Atmospheric and Oceanic Technology*, 32, 177-184.

Acknowledgements

This study is a contribution to the SWOT science team and was conducted during a one month internship of L. Gómez-Navarro at IMEDEA (CSIC-UIB) under the supervision of E. Mason and A. Pascual, in the frame of her Master in Marine Physics.
L. Gómez-Navarro acknowledges the support of CNES in the form of a travel grant, which enabled her to attend this colloquium.
Evan Mason is supported by a post-doctoral grant from the *Conselleria d'Educació, Cultura i Universitats del Govern de les Illes Balears* (Mallorca, Spain) and the European Social Fund.
The authors acknowledge the help of L. Gaultier for implementing the SWOT simulator and her insight when problems were encountered and the help of Francisco Eugenio of the remote-sensing department of the University of Las Palmas de Gran Canaria for the chlorophyll satellite images.
NASA Goddard Space Flight Center, Ocean Ecology Laboratory, Ocean Biology Processing Group; 2012: VIIRS-NPP Data; NASA Goddard Space Flight Center, Ocean Ecology Laboratory, Ocean Biology Processing Group. Accessed on 01/03/2016.

Govern de les Illes Balears